Electronic Supporting Information

for

High-Sensitivity Detection of Dopamine by Biomimetic Single Nanochannels Modified with Amine-appended Polyaniline

Gregorio Laucirica,[1†] Yamili Toum Terrones,[1†] Vanina M. Cayón,[1] M. Lorena Cortez,[1] María Eugenia Toimil-Molares,[2] Christina Trautmann,[2,3] Waldemar A. Marmisollé[1]* and Omar Azzaroni[1]*

[1]Instituto de Investigaciones Fisicoquímicas Teóricas y Aplicadas (INIFTA), Departamento de Química, Facultad de Ciencias Exactas, Universidad Nacional de La Plata, CONICET – CC 16 Suc. 4, 1900 La Plata, Argentina

[2]GSI Helmholtzzentrum für Schwerionenforschung, 64291 Darmstadt, Germany

[3]Technische Universität Darmstadt, Materialwissenschaft, 64287 Darmstadt, Germany

[†] These authors contributed equally to the work

[*] E-mail: wmarmi@inifta.unlp.edu.ar (W.A.M.)
E-mail: azzaroni@inifta.unlp.edu.ar (O.A.)

S.1. PABA characterization

NMR

^{1}H-NMR spectra were acquired for the ABA monomer and for the reaction product after polymerization (50 mM solution of ABA, 1.5 hours) in D_2O, as reported by Marmisollé *et al.*[1] As shown in **Figure S1 (a)**, for ABA, there is a signal at 3.62 ppm (singlet, 2 H) that belongs to the protons of the methylene group in the benzylamine moiety (H1, H2). Furthermore, ABA has two aromatic signals at 6.71 (multiplet –m-) and 7.14 ppm (triplet –t-) that belong to the 4 non-equivalent aromatic protons of the molecule.

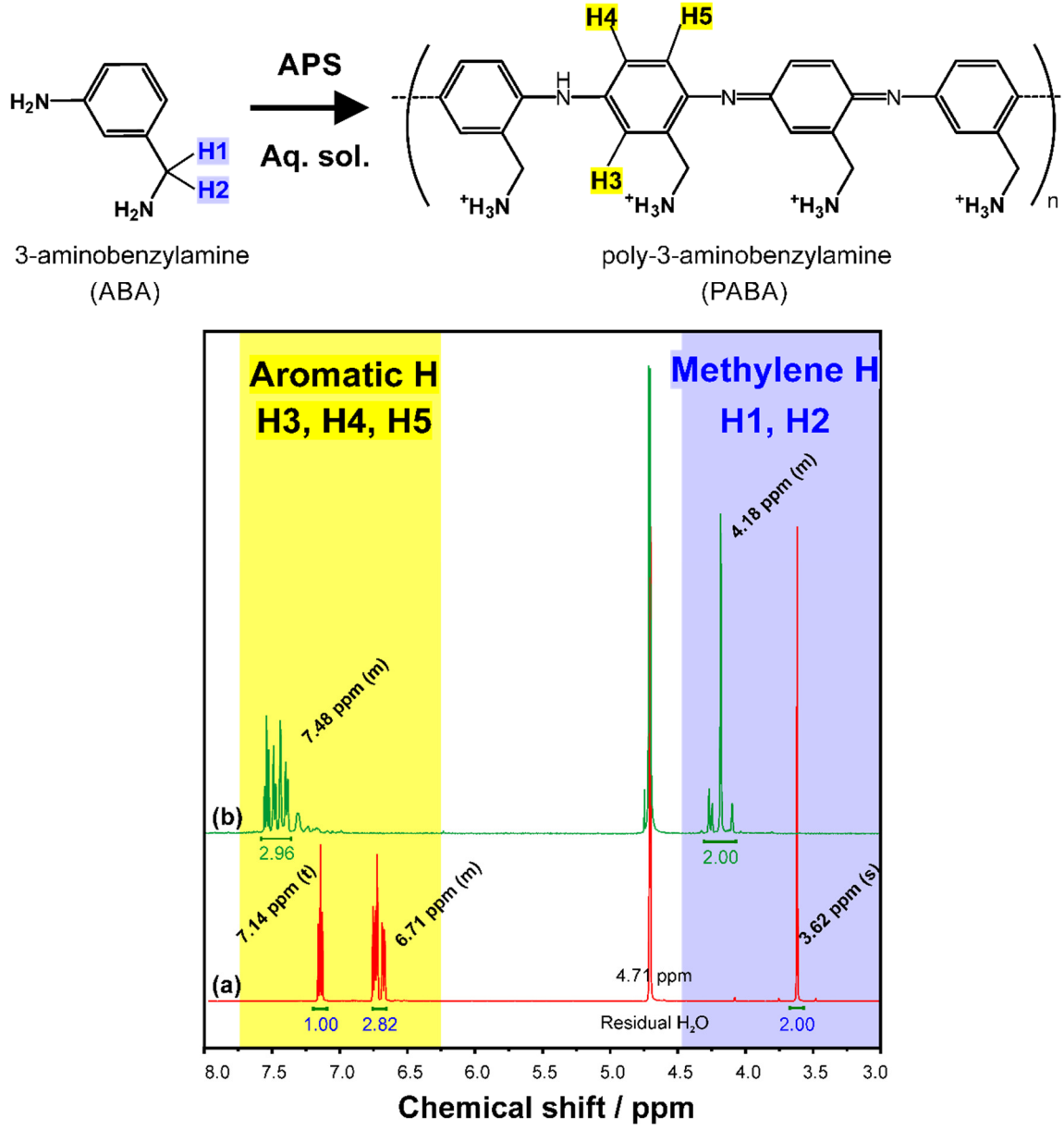

Figure S1. 500 MHz ^{1}H NMR spectra (D_2O) of ABA monomer **(a)** and PABA **(b)** synthesis reaction mixture. The different types of protons in the chemical structures are marked to guide the reader.

During the polymerization, covalent bonds C-N-C are formed to build the polymer, and consequently, one of the four aromatic protons of ABA is lost for each new bond. Then, only the non-equivalent protons H3, H4, and H5 correspond to the multiplet signal at 7.48 ppm. As calculated from the integrals of **Figure S1**, the ratio H (aromatic)/H(methylene) changes from 2 in ABA **(a)** to 1.5 in PABA **(b)**.

After adding the oxidizing agent APS, polymerization takes place accompanied by a pH decrease and a broadening of both aliphatic and aromatic proton signals as well as a shift to higher chemical shifts. As discussed by Marmisollé *et al.*, this effect is related to the protonation of both aromatic and benzyl amino groups at lower pH values.[1]

IR spectroscopy

Fourier transform infrared spectroscopy in the attenuated total reflection mode (ATR-FTIR) was performed using a Varian 600 FTIR spectrometer equipped with a ZnSe ATR crystal with a resolution of 4 cm^{-1}. Background-subtracted spectrum was corrected for ATR acquisition by assuming a refractive index of 1.52. **Figure S2**¡Error! No se encuentra el origen de la referencia. shows the ATR-FTIR spectrum of a PABA deposited on a gold substrate from a 0.5 HCl solution by drop-casting. The substrate was allowed to dry at room temperature for 48 hs before measuring.

Table S1. Assignments of the main ATR-FTIR bands of PABA deposited from HCl solution.

ν / cm^{-1}	**Assignments**
690	C-H out of plane bending of 1,2-substituted benzenic units[2]
830	C-H out of plane bending of p-substituted benzenic units [2,3]
1000	C-H in plane bending[2]
1120	N=Q=N stretching,[4,5] stretching of Q=NH+-B in the doped form;[2] C-H bending in aromatic units[5,6]
1250	C=N=C stretching[3–5]; sym. C-N stretching[6]
1360	C-N stretching [2,3]
1450	C-C aromatic stretching;[5] C-N stretching[3]
1490	N-B-N stretching;[2] C-C in benzenic units;[3,4] N-H bending;[4] Q=N-B stretching[3]
1585	N=Q=N stretching,[2–5]
2930	Methylene stretching[7]
3350	Broad band due to H-bonded NH stretching[5]

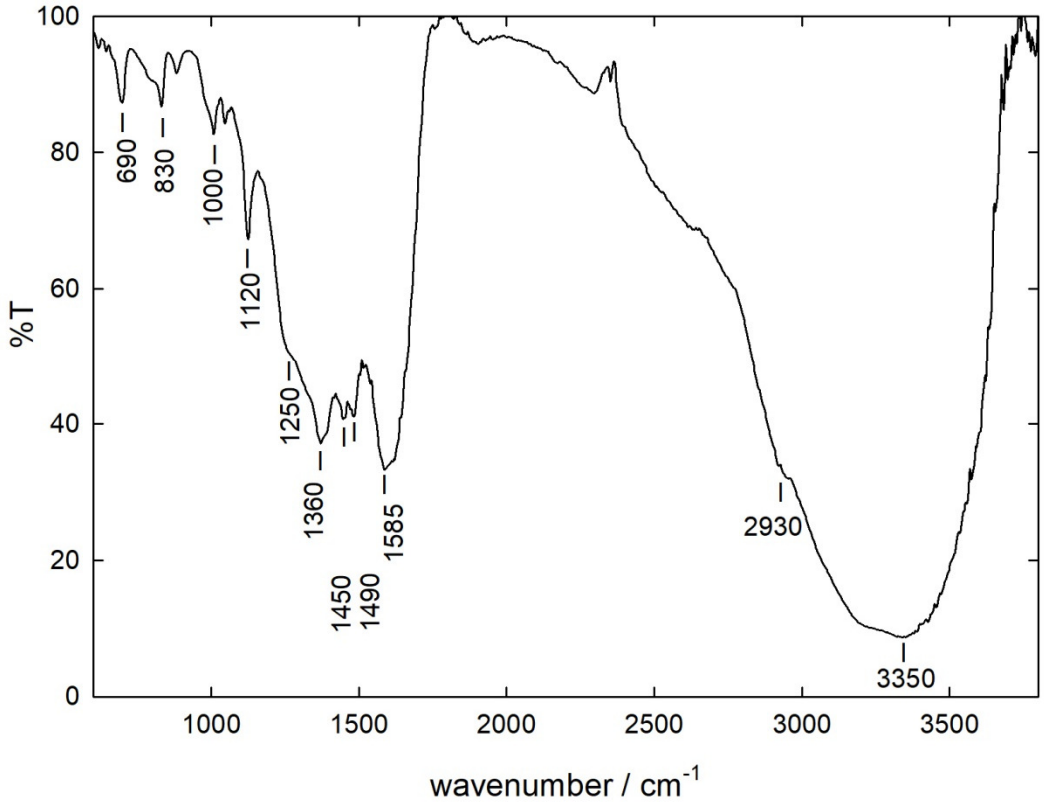

Figure S2. ATR-FTIR spectrum of PABA deposited on Au substrate from aqueous acidic solution.

S.2. Nanochannel characterization by field emission scanning electron microscopy (FE-SEM) imaging

Bullet-shaped nanochannels were characterized by FE-SEM imaging (**Figure S3**). For this aim, a 12 µm thick PET foil irradiated with 10^9 ions cm^{-2} was subjected to an asymmetrical surfactant-assisted etching (60 °C, 6 minutes).[8] In order to obtain cross-section images, the multi-pore membrane was treated with UV irradiation and liquid N_2. Then, it was mechanically broken. The images revealed parallel oriented channels with the typical bullet-shaped pore opening at the membrane surface. The base had a diameter of around ~900 nm.

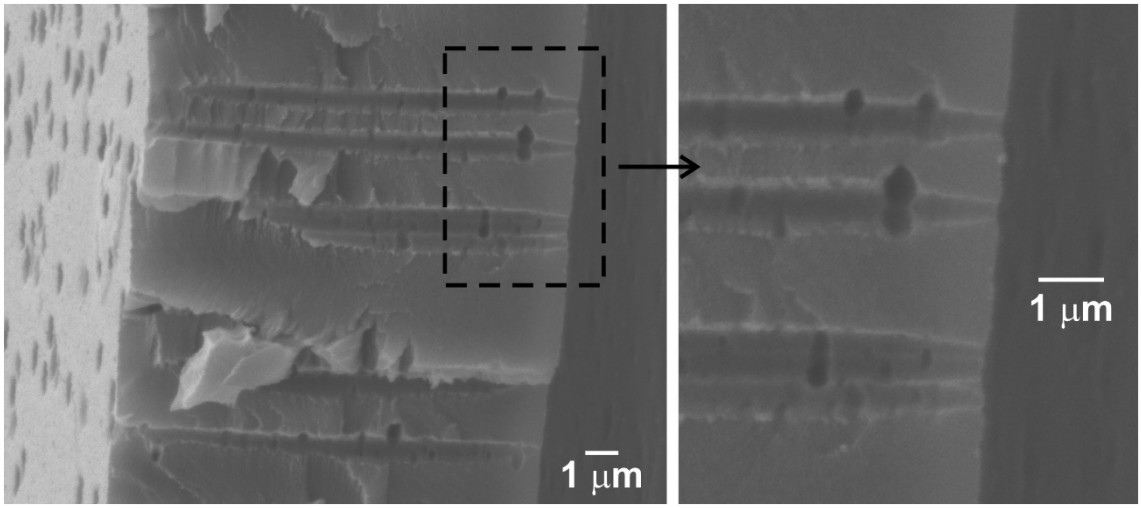

Figure S3. Cross-section FE-SEM image of PET membrane with the bullet-shaped nanochannels.

Using the base diameter obtained by SEM, the tip diameter we estimated to be ~20 nm. This value was deduced from channel conductance measurements performed at high ionic strength (1 M KCl) and low transmembrane potential (calculation details are available in reference 9). The curvature parameter *h* was assumed to be 1500 nm from the bibliography.[10]

S.3. Experimental set-up

Conductimetric measurements were carried out in a electrolytic cell using a potentiostat with a four-electrode arrangement (**Figure S4**) consisting of the working electrode W (Pt wire), the two reference electrodes WS and R (Ag/AgCl/3 M KCl) and a counter electrode CE (Pt wire). In all experiments, W and WS were placed in the chamber facing the tip side of the foil.

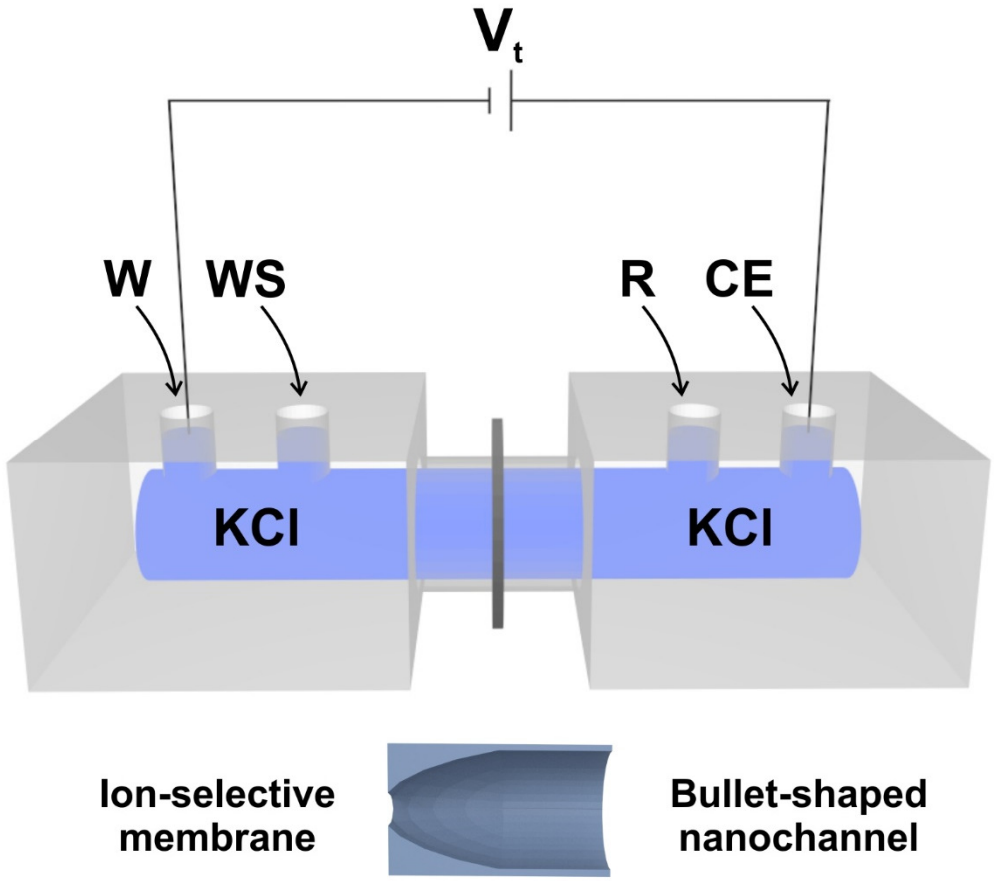

Figure S4. Scheme of experimental set-up used for the iontronic (not to scale) measurements consisting of two chambers separated by a PET membrane containing one single bullet-shaped nanochannel. The ionic flow of the KCl electrolyte through the nanochannel is monitored by a potentiostat with four-electrodes (working electrode W, working sense WS, reference R, counter-electrode CE).

S.4. Control transport experiments

As shown in the main text, the immersion of a PET/PABA foil in a dopamine solution (DA, pH=9) for 30 minutes leads to a decrease in rectification efficiency (f_{rec}). In order to ascribe the ion transport changes to the interaction DA-PABA, required appropriate control experiments (**Figure 5**). In a first step, a bare PET channel was exposed to DA under the same conditions as PET/PABA channels presented in the main text (**Figure 5 (a)**). Both the measurements before and after DA exposition are characterized by ohmic transports due to the low ratio of dissociated carboxylate groups of PET at pH=3. Additionally, I-V curves (DA 0 µM and DA 1 µM)

show that the DA treatment does not cause any significant changes in the iontronic output. This fact suggests that there is no interaction between PET and DA under the given conditions, a crucial point to take into account. On the other hand, the same treatment conditions that those used in the main text to test the DA-responsiveness (mQ water, pH 9, 30 minutes) were again applied to the modified channel but in absence of DA. This experiment allows to evaluate possible desorption of PABA from the surface promoted by the basic treatment conditions. The exposure to pH 9 did not cause significant changes in the iontronic output, whereas the subsequent exposition to 1 nM DA triggered a clear change in the response. Thus, these experiments support the idea that DA acts as a chemical effector through a specific chemical reaction between the primary amine groups of immobilized PABA and the oxidized form of DA at pH 9.

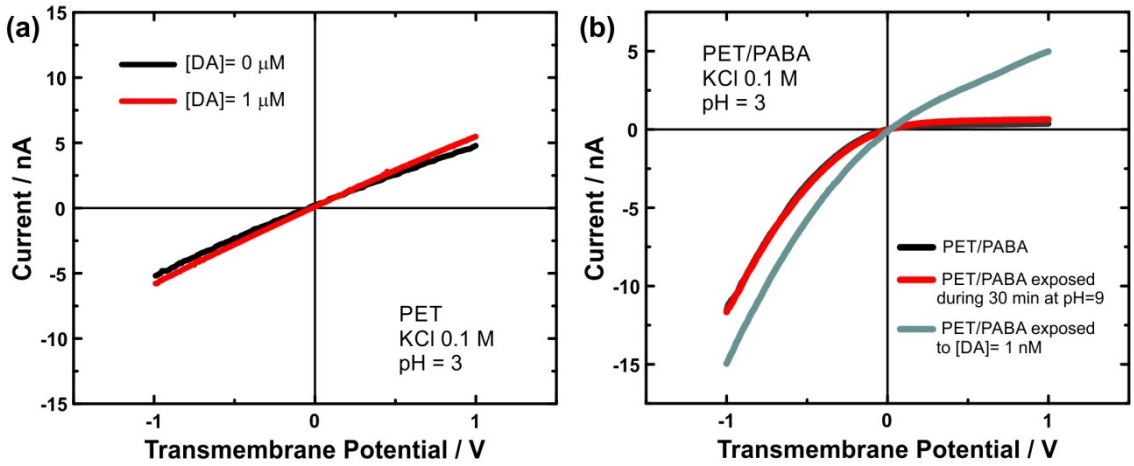

Figure S5. Iontronic transport of **(a)** a bare PET channel before (black) and after (red) exposition to DA and **(b)** a PET/PABA SSN before (black) and after (red) exposition to mQ water pH=9 together with the response of PET/PABA SSN after exposition to 1 nM DA (grey). In all cases, measurements were carried out in 0.1 M KCl at pH=3.

S.5. Binding Model for the iontronic Dopamine responsiveness

For interpreting the DA-responsiveness of the PET/PABA SSN, we developed a binding model in which the sensoring process is deconvoluted into a first chemical binding process taking place in the presence of DA at pH 9 and a subsequent analysis of the iontronic characteristic taking place at pH 3 without DA in solution (see **Scheme S1**). The main idea behind the analysis is that the binding equilibrium situation is frozen at pH 9 when changing the pH of the solution for the iontronic readout.

Firstly, let us consider the association between DA and amine groups from PABA at pH=9 as a binding problem. This means it is possible to write The equilibrium equations for this chemical interaction can be written as[11]

$$(R-NH_2)+DA \leftrightarrow (R-NDA) \qquad K_{DA} \qquad \text{(S.1)}$$

$$K_{DA}=\frac{\left[(R-NDA)\right]}{\left[(R-NH_2)\right]\left[DA\right]} \qquad \text{(S.2)}$$

where agents in round braquets mean surface groups whereas [DA] refers to its bulk concentration and K_{DA} can be considered a binding constant.

After soaking in the DA solutions, the PET/PABA SSN membranes are measured in a DA-free 0.1 KCl solution of pH 3. However, the fraction of the amine surface groups bound to DA remains at pH 3 as the reaction is not reversible under that operating condition. Then, the consequence of the previous immersion in DA is an irreversible transformation of a fraction of the R-NH_2 groups to R-NDA. Let Γ_{NH_2} be the total concentration of amine surface groups from PABA, then

$$\frac{\left[(R-NH_2)\right]}{\Gamma_{NH2}}=\frac{1}{(1+K_{DA}\left[DA\right])} \qquad \text{(S.3)}$$

$$\frac{\left[(R-NDA)\right]}{\Gamma_{NH2}}=\frac{K_{DA}\left[DA\right]}{(1+K_{DA}\left[DA\right])} \qquad \text{(S.4)}$$

where expressions (S.3) and (S.4) correspond to the fraction of unmodified and DA-bound amine sites after being exposed to the DA solution, respectively.

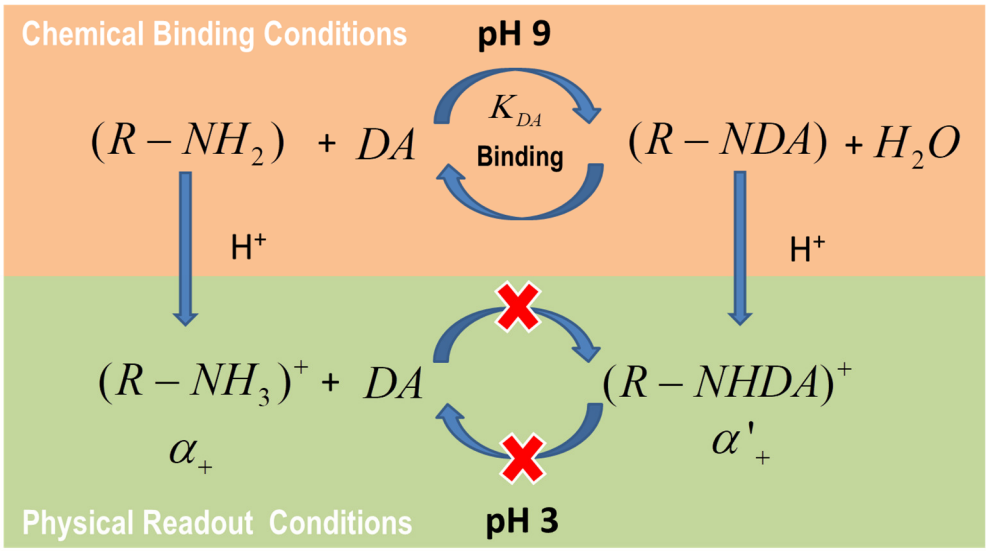

Scheme S1. Chemical species and steps used for interpreting the DA-responsiveness in terms of a simple binding model.

At acidic conditions of the iontronic measurements (pH 3), a fraction α_+ of the unmodified amine groups in PABA will be protonated. In principle, a fraction α'_+ of the DA-modified sites could also be protonated. According to the chemical structures, it is expected that $\alpha_+ >> \alpha'_+$. **Scheme S1** summarizes the main features of the binding model.

On the other hand, the presence of negative charges from carboxylates surface groups of the etched PET SSN walls can be neglected at pH 3.[12] Thus, the surface charge density (σ) can be computed by taking into account the contribution of protonated free and DA-bound amine groups,

$$\sigma \propto \alpha_+[(R-NH_2)] + \alpha'_+[(R-NDA)] \qquad \text{(S.5)}$$

By employing relations (S.3) and (S.4), we obtain

$$\sigma \propto \frac{\alpha_+ + \alpha'_+ K_{DA}[DA]}{(1+K_{DA}[DA])} \qquad \text{(S.6)}$$

Before exposition to DA solutions, the surface charge density at pH 3 corresponds to the protonated amine groups from PABA, then

$$\sigma_0 \propto \alpha_+ \qquad \text{(S.7)}$$

On the other hand, when high DA concentrations are employed, a saturation behavior appears. The surface charge density observed at pH 3 comes from the contribution of the DA-bound moieties, so

$$\sigma_{\infty} \propto \alpha'_{+} \qquad \text{(S.8)}$$

Then, expression (S.6) can be rewritten to

$$\sigma = \frac{\sigma_0 + \sigma_{\infty} K_{DA}[DA]}{(1 + K_{DA}[DA])} \qquad \text{(S.9)}$$

and

$$\frac{\sigma}{\sigma_0} = \frac{1 + \frac{\sigma_{\infty}}{\sigma_0} K_{DA}[DA]}{(1 + K_{DA}[DA])} \qquad \text{(S.10)}$$

Changes in the surface charge density can be correlated with changes in the rectification factors. Particularly, it has been proved that for a low surface charge, there is a linear relationship between σ and f_{rec}, which allows writing[12]

$$\frac{f_{rec}}{f_{rec}^0} = \frac{\sigma}{\sigma_0} = \frac{1 + \beta K_{DA}[DA]}{1 + K_{DA}[DA]} \qquad \text{(S.11)}$$

with f_{rec}^0 being the initial value, before exposition to DA, and β is defined as

$$\beta = \frac{f_{rec}^{\infty}}{f_{rec}^0} = \frac{\alpha'_{+}}{\alpha_{+}} \qquad \text{(S.12)}$$

where f_{rec}^{∞} is the rectification factor measured after exposition to high binding DA concentrations. This parameter β is a measure of the differential protonation degree caused by the DA functionalization.

References

1 W. A. Marmisollé, E. Maza, S. Moya and O. Azzaroni, *Electrochim. Acta*, 2016, **210**, 435–444.

2 J. Tang, X. Jing, B. Wang and F. Wang, *Synth. Met.*, 1988, **24**, 231–238.

3 Y. Furukawa, F. Ueda, Y. Hyodo, I. Harada, T. Nakajima and T. Kawagoe, *Macromolecules*, 1988, **21**, 1297–1305.

4 J. Laska and J. Widlarz, *Polymer (Guildf).*, 2005, **46**, 1485–1495.

5 C. Sanchís, H. J. Salavagione, J. Arias-Pardilla and E. Morallón, *Electrochim. Acta*, 2007, **52**, 2978–2986.

6 M.-I. Boyer, S. Quillard, E. Rebourt, G. Louarn, J. P. Buisson, A. Monkman and S. Lefrant, *J. Phys. Chem. B*, 1998, **102**, 7382–7392.

7 B. L. Rivas and C. O. Sánchez, *J. Appl. Polym. Sci.*, 2004, **92**, 31–36.

8 P. Y. Apel, I. V. Blonskaya, S. N. Dmitriev, O. L. Orelovitch, A. Presz and B. A. Sartowska, *Nanotechnology*, 2007, **18**, 305302.

9 G. Laucirica, W. A. Marmisollé, M. E. M. E. Toimil-Molares, C. Trautmann and O. Azzaroni, *ACS Appl. Mater. Interfaces*, 2019, **11**, 30001–30009.

10 G. Laucirica, A. G. Albesa, M. E. Toimil-Molares, C. Trautmann, W. A. Marmisollé and O. Azzaroni, *Nano Energy*, 2020, **71**, 104612.

11 G. Laucirica, W. A. Marmisollé and O. Azzaroni, *Phys. Chem. Chem. Phys.*, 2017, **19**, 8612–8620.

12 G. Pérez-Mitta, A. Albesa, F. M. Gilles, M. E. Toimil-Molares, C. Trautmann and O. Azzaroni, *J. Phys. Chem. C*, 2017, **121**, 9070–9076.